ACS OMEGA

http://pubs.acs.org/journal/acsodf

Article

Novel PFA-Based Inorganic Three-Phase Foam for Inhibiting Coal Spontaneous Combustion

Jian Chen, Baoshan Jia,* Shuoqin Fu, Ying Wen, Yuntao Liang, and Fuchao Tian

Cite This: *ACS Omega* 2023, 8, 24615−24623

Read Online

ACCESS | Metrics & More | Article Recommendations

ABSTRACT: Fire accidents caused by coal spontaneous combustion usually lead to a large loss of coal resources and casualties. Not only that, the greenhouse effect is polluted while the environment is polluted. At present, the commonly used fire-extinguishing materials such as water, inhibitors, and organic foams have the disadvantages of poor stability and short fire-extinguishing cycles. It is difficult to effectively suppress coal spontaneous combustion and quickly extinguish the fire for a long time. To suppress the spontaneous combustion of coal, the research team proposed an inorganic three-phase foam with a high foam expansion rate, good cohesiveness, and excellent stability. In the formulation, pulverized fly ash (PFA) is used as the matrix, sodium dodecyl benzene sulfonate (SDBS) and α-olefin sulfonate (AOS) are used as foaming agents, curdlan is used as the foam stabilizer, and sodium silicate is the binder. The compound foaming agent with the best performance is optimized, through the two-group compounding test. The composite foaming agent's optimal compound ratio is SDBS/AOS (3:2). The optimal ratio of inorganic three-phase foam (ITPF) components was obtained through the control variable method experiment. The water−cement ratio is 5:1, the composite foaming agent is 0.2%, the curdlan is 0.5%, and the sodium silicate is 1.6%. In addition, it has been determined by experiments that ITPF has the strongest foaming ability when the pH value is 9 and the temperature is 60 °C. The fire-extinguishing performance of the new material ITPF was investigated by thermogravimetry and coal spontaneous combustion tendency test. It has been observed that the new material has the effect of cooling down and isolating coal from contact with oxygen. The results show that the new material ITPF has the potential to prevent coal spontaneous combustion.

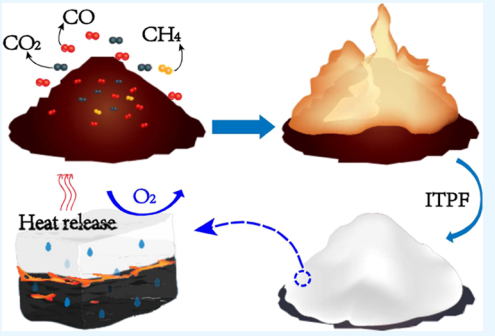

1. INTRODUCTION

Coal is the main energy source that dominates the global economy.[1,2] Coal has always played an important role in the fields of power generation, steel, and chemical industry.[3−5] China is a big coal-consuming country, and coal consumption will still dominate in the next few years. Coal spontaneous combustion has always been one of the main threats to coal mine safety. The resulting fire will cause casualties, heavy property losses, and serious environmental pollution.[6−8] First of all, coal spontaneous combustion has been going on for decades, even centuries in some areas, such as coal-producing areas in northwest China, India, and Bangladesh. These areas are dry and rainless, and the ecology is fragile. The high temperature caused by the spontaneous combustion of coal evaporates the surrounding groundwater, rivers, and lakes, further destroying the ecological environment. Second, surveys show that billions of tons of coal resources, worth hundreds of billions of dollars, are lost each year due to coal spontaneous combustion. Finally, coal spontaneous combustion produces a large amount of toxic and harmful gases such as CO, CO_2, C_2H_4, SO_2, etc., which intensifies the greenhouse effect.[9,10]

In recent years, with the increase of coal mine mining depth, the temperature of coal mines underground has increased accordingly. At the same time, the ground stress also increases. Therefore, the remaining and broken coal bodies in the goaf are affected by this, and the degree of fragmentation and spontaneous combustion tendency of coal also increases. Oxidation and spontaneous combustion of coal are more frequent. As a result, the occurrence frequency and damage degree of spontaneous combustion disasters in deep coal mines are significantly higher than those in shallow mines.[11−13] Therefore, it is considered from the aspects of resource conservation, environmental protection, and safe mining. Efficient coal mine fire prevention and extinguishing technical measures to prevent coal spontaneous combustion are imminent.[14−16]

To prevent and control the occurrence and spread of coal mine fires, domestic and foreign scholars have studied different

Received: April 26, 2023
Accepted: June 8, 2023
Published: June 26, 2023

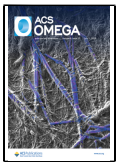

ACS Publications

© 2023 The Authors. Published by American Chemical Society

https://doi.org/10.1021/acsomega.3c02881
ACS Omega 2023, 8, 24615−24623

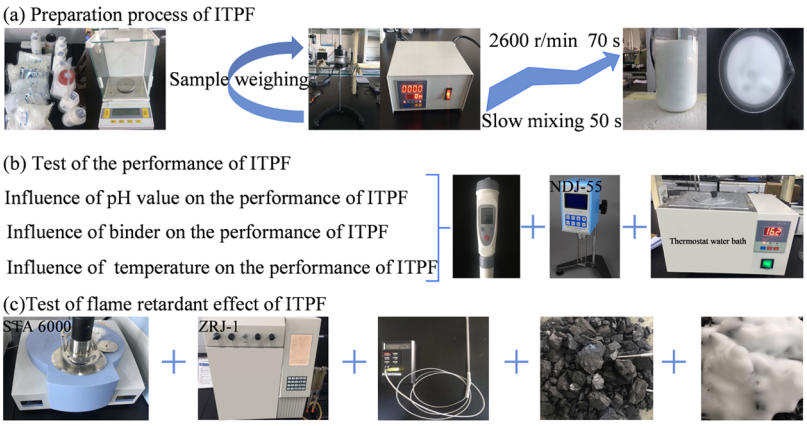

Figure 1. Experimental design scheme and flow chart.

fire prevention and fire-extinguishing technologies to prevent coal spontaneous combustion since the 1950s. For example, measures[17] such as plugging, pressure equalization, water injection,[18] inert gas, grouting,[19] foam injection,[16,20,21] gel spraying, and corrosion inhibitor aerosols have been gradually proposed and widely used. The above technical measures have played an important role in the prevention and control of coal spontaneous combustion. However, these measures still have some shortcomings.[22,23] In the process of water injection and grouting, water and mud only flow from high to low water levels along the ground.[24,25] Gels are usually poorly mobile, have a small diffusion range, and tend to break.[20,26] The foam is easy to lose water and has poor stability. To overcome the above shortcomings, new foam fire prevention technology has attracted increasing attention due to its excellent fluidity, accumulation ability, and high stability.[27] Scholars at home and abroad have done a lot of research on the preparation and fire-extinguishing mechanism of flame-retardant foam.

Zhi[28] et al. proposed a new type of composite colloid to prevent the spontaneous combustion of coal, which can increase the critical temperature of coal, the average activation energy, and the isolation of oxygen and effectively inhibit the spontaneous combustion reaction of coal. Zhang[29] et al. developed an alginate fluid gel (AFG)-stabilized clay aqueous suspension, which can increase the cross-point temperature and reduce CO release, effectively inhibiting the spontaneous combustion of coal. Qin[30] et al. have developed a new, three-dimensional, stable, and excellent clay suspension, which can improve the thermal stability and cross-point temperature (CPT) of coal and effectively inhibit the spontaneous combustion of coal. Wang[31] et al. proposed a new type of composite material foaming gel with high water absorption and excellent fire resistance. The foaming gel can effectively seal leaks, effectively reduce coal temperature, and inhibit coal oxidation reaction rate and heating rate. Xi[32] et al. developed a novel solid waste-based composite foam for the prevention and control of coal spontaneous combustion, which has the advantages of good airtightness, low thermal conductivity, and high fire-extinguishing efficiency. Xue[33] et al. successfully prepared gel foam using water glass, coagulant, modified polyoxyethylene ether silicone, and composite blowing agent. Gel foam significantly reduces ignition temperature, heat radiation, and CO emissions. Guo[34] et al. prepared gel foam by using condensed aluminum phosphate, sodium dodecyl benzene sulfonate (SDBS), FAPES, and other materials. Compared with pure foam, the gel foam has a lower water loss rate and better stability and exhibits excellent fireproof performance. Xi[35] et al. prepared a new type of polycrystalline gel foam using sodium silicate, polycaprolactone, polyethylene oxide, and organic acids. The formation of $-CH_2/CH_3$ and $-OH$ functional groups during low-temperature oxidation of coal was strongly suppressed. Previous studies have proved that foam has an irreplaceable and excellent effect in preventing the spontaneous combustion of coal.[36−38] However, the foam or gel commonly used in coal mines still has disadvantages such as poor fire-extinguishing effect, high material cost, poor stability, harm to human health, and damage to the ecological environment.[39] In particular, there are potential fire sources and high fire source control problems in fully mechanized caving goaves and roadway high-release areas. In particular, the potential fire source and high fire source control problems in the upper and lower layer mining composite gobs and the air inlet and return airways. Therefore, in response to the actual needs of coal mine site safety products, it is of great significance to develop a batch of new environmentally friendly fire-fighting three-phase foams with excellent fire-fighting properties. Materials used in this paper include pulverized fly ash (PFA), blowing agents sodium dodecyl benzene sulfonate (SDBS) and α-olefin sulfonate (AOS), foam stabilizer curdlan and adhesive agent sodium silicate (SS), and water. A new type of environmentally friendly inorganic three-phase foam (ITPF) with foam as the carrier has been developed. Through optimization and compounding tests, the best compounding ratio to achieve the best foam expansion rate, stability, and fire-extinguishing effect is obtained. In addition, experimental instruments such as a dispersive X-ray spectrometer, probe-type thermocouple digital display high-precision temperature measuring instrument, comprehensive thermal analyzer STA6000, and ZRJ-1 coal spontaneous combustion tester were used to test the performance of ITPF. The fire-extinguishing mechanism of the new foam was discussed from the aspects of the temperature change law of the coal pile, the thermal weight loss rate, and the oxygen absorption of the coal. This study proposes a novel inorganic three-phase foam based on a composite blowing agent and PFA. This material was found to be effective in preventing and delaying the burning of coal. ITPF has the following three advantages compared with existing foams: (1) The main components of ITPF are PFA, SDBS, AOS, curdlan, SS, and water, which have no impact on the ecological environment. (2) ITPF has a high expansion ratio, stability, and cohesiveness. (3) ITPF contains

https://doi.org/10.1021/acsomega.3c02881
ACS Omega 2023, 8, 24615−24623

flame-retardant ingredients, which have good performance in preventing coal spontaneous combustion.

2. MATERIALS AND EXPERIMENTAL METHODS

A variety of single-foaming agents with excellent performance were selected, and compound tests were designed. The influence of the water−cement ratio, pH value, and temperature on the performance of ITPF was analyzed. ITPF was prepared according to the optimal material ratio. The performance of ITPF in preventing coal spontaneous combustion was investigated from the aspects of thermal weight loss rate, coal spontaneous combustion tendency, and flame-retardant effect. The overall test design scheme is shown in Figure 1.

2.1. Materials. Materials for producing ITPF are as follows. The formula uses PFA as the matrix, SDBS and AOS as the foaming agents, curdlan as the foam stabilizer, and SS as the binder. The particle size distribution range of PFA particles is below 300 μm. PFA is the main solid waste discharged from coal-fired power plants as the main material of ITPF aggregate. The specific composition of PFA is shown in Figure 2.

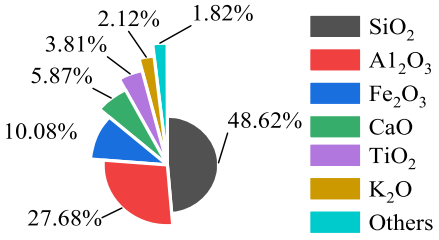

Figure 2. Chemical composition and proportion of PFA.

Industrial solid waste can be turned into treasure if PFA can be used to make fire prevention material ITPF.[40−44] The benefits of comprehensive utilization of coal resources will be greatly improved.

2.2. Method of Compounding Test. *2.2.1. Preference Test for a Single-Foaming Agent.* First, the properties of 10 blowing agents are analyzed using experimental comparison. The concentration of the foaming agent solution is fixed at 0.5%. Each group of experiments was repeated 3 times, and the average value was calculated.

2.2.2. Determining the Best Combination and Ratio of Compound Foaming Agent (CFA). According to the results of (1) test, a two-group compound test program was designed. The concentration of the fixed composite blowing agent solution is 0.1%, and the concentration of the foam stabilizer is 0.2%. The optimal compounding ratio among the six ratios of 5:0, 4:1, 3:2, 2:3, 1:4, and 0:5 was explored.

2.2.3. Determining the Optimal Concentration of a Compound Blowing Agent. According to the test results of 2.2(2), the compounding ratio of two groups was set. At the same time, the water−cement ratio is fixed at 3:1, the concentration of foam stabilizer is 0.2%, and the volume of the mixed solution is 50 mL. On this basis, a two-group compound experiment was carried out. The compound foaming agent was prepared with concentrations of 0.1, 0.2, 0.3, 0.4, and 0.5%, respectively, and the effect of CFA concentration on the maximum foaming volume was studied. The experiment was repeated 3 times to reduce the experimental error.

2.3. Trials for ITPF Performance Testing. The performance test of ITPF mainly includes the influence of foam stabilizer, binder, water−cement ratio, pH value, and temperature on the performance of ITPF, as shown in Figure 1b.

The fire prevention and extinguishing performance test of ITPF includes a thermogravimetric test and a coal spontaneous combustion tendency test, as shown in Figure 1c.

2.3.1. Foam Stabilizer Test. The optimum CFA concentration is set to 0.2%, the water−cement ratio is 3:1, and the solution volume is 50 mL. The effect of different concentrations of foam stabilizer Curdlan on foam performance was studied.

2.3.2. Adhesive Test. Using an NDJ-55 rotational viscometer, the viscosity of foam was measured when adding different concentrations of sodium silicate aqueous solution (SSAS). The variation curve of foam viscosity with SSAS concentration and time was investigated, and it was recorded every 120 s. Furthermore, the change law of ITPF foam properties under different SSAS concentrations was studied. The CFA concentration was set at 0.2%, and the water−cement ratio was 3:1. The concentrations of SSAS were 0, 1, 1.2, 1.4, 1.6, 1.8, and 2.0%, respectively. At the same time, SSAS with zero addition was set as the reference group, and the foaming time was 2 min. The maximum foaming volume V_{max} of ITPF was recorded under different SSAS concentrations. When the fixed volume of the foam is 500 mL, its drainage half-life is recorded.

2.3.3. Water−Cement Ratio Test. To study the effect of different water−cement ratios on the foaming effect, the CFA concentration was set at 0.2%, the SSAS concentration at 1.6%, and the water−cement ratio at 3:1, 4:1, 5:1, and 6:1, respectively. The foaming time and foaming volume were set to 2 min and 500 mL, respectively.

2.3.4. pH Test. The CFA concentration, binder SSAS concentration, and water−cement ratio were set to be 0.2, 1.6%, and 5:1, respectively. The maximum foaming volume of ITPF within 120 s was studied under different pH values (3−11) by using a pH measuring instrument, and at the same time, the amount of liquid dripping of ITPF under the same foaming volume was tested.

2.3.5. Temperature Test. The initial temperature of the constant temperature water bath (CTWB) was set at 20 °C. The measuring beaker containing the prepared foam is placed in CTWB, and when the temperature is stable, take out the beaker, read, and record. The temperature was measured every 10 °C, and the cycle was repeated until the test was stopped at 100 °C, as shown in Figure 1a,b.

2.3.6. Thermogravimetric Test. Three coal samples of the same mass were weighed with a balance with a sensitivity of 0.1 μg and dried by vacuum drying. Raw coal, AOS + coal, and ITPF + coal were tested by a comprehensive thermal analyzer STA6000 in a nitrogen atmosphere with an oxygen concentration of 20.9%. The initial temperature of the test was set at 30 °C, the maximum temperature was 800 °C, and the heating rate was 10 °C/min.

2.3.7. Coal Spontaneous Combustion Tendency Test. In this experiment, the oven temperature of the ZRJ-1 Coal Spontaneous Combustibility Tester (CSCT) is set at 30 °C, and the thermal conductivity temperature is 80 °C. The empty tube adsorption time is 5 min, the empty tube gas carrying capacity is 32 cm^3/min, and the empty tube adsorption gas flow rate is 20 cm^3/min. Raw coal, AOS + coal, and ITPF + coal were tested by CSCT to obtain the coal oxygen uptake of the three coal samples.

https://doi.org/10.1021/acsomega.3c02881
ACS Omega 2023, 8, 24615−24623

3. RESULTS AND DISCUSSION

3.1. Results and Analysis of Foaming Agent Optimization. *3.1.1. Single-Foaming Agent Optimization Results and Analysis.* The maximum foam volume V_{max} and the half-life of liquid drainage T_{half} of four types of 10 single foaming agents (SFA) were obtained through experiments, as shown in Figure 3. It can be seen from Figure 3 that the foam

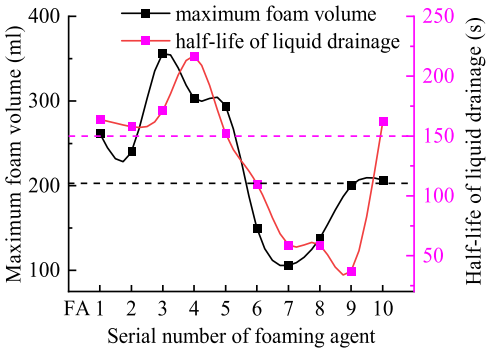

Figure 3. Foam volume and drainage half-life curves of a single blowing agent.

expansion performance and half-life of liquid drainage of different SFAs are quite different. Based on comprehensive analysis and comparison of test results, six blowing agents FA1−FA5 and FA10 with relatively good performance were selected. Their maximum foaming volume V_{max} is greater than 203 mL, and the half-life of liquid drainage T_{half} is greater than 150 s, as shown in Table 1 and Figure 3.

Table 1. Serial Number, Name, and Type of a Single Blowing Agent

serial number	name of the blowing agent	category
FA 1	sodium dodecyl benzene sulfonate SDBS	anion
FA 2	fatty alcohol polyoxyethylene ether sulfate FAPES	
FA 3	sodium *n*-lauroyl sarcosinate SNLS	
FA 4	*α*-olefin sulfonate AOS	
FA 5	benzyldodecyldiMethylaMMoniuM broMide BB	cation
FA 6	fatty alcohol polyoxyethylene ether FAPE	nonionic
FA 7	lauryl glucoside LG	
FA 8	fatty acid methyl ester ethoxylates FAMEE	
FA 9	dodecyl dimethyl betaine DDB	amphoteric
FA 10	cocoamidopropyl betaine CB	

3.1.2. Optimization Results and Analysis of a Compound Blowing Agent. The six blowing agents screened out are compounded in pairs according to the set ratio. A, B, C, D, E, and F correspond to foaming agents SDBS, CB, FAPES, BB, SNLS, and AOS, respectively. The foam volume and drainage half-life of the compound foaming agent under different compound ratios are shown in Figures 4 and 5. As shown in Figures 4 and 5, there are four groups A, B, C, and E. The compound solutions of other groups could not form foam through high-speed stirring, and the drainage half-life could not be measured. Due to the synergistic effect of the two-component compound, the foam performance of the compound blowing agent is far superior to that of a single blowing agent, as shown in Figures 3−5. In addition, under the test conditions, the performance of the compound foaming agent increases first and then decreases with the change in the ratio. The ratio of the two-group compound blowing agent (CFA) is determined to be A/F (3:2), and the concentration of the compound blowing agent is 0.2%. Under the above parameters, CFA has the best foaming ability and foam stability and the best overall performance.

The change curve of foam volume with the change in CFA concentration is shown in Figure 6. It was observed that there was no significant difference in the results of the three repeated tests. The change in foam volume showed a trend of first increasing and then decreasing. When the concentration of CFA is 0.2%, the foam volume is the largest. When the CFA concentration exceeds 0.2%, the foam volume begins to decrease gradually. Therefore, the optimal concentration of CFA was determined to be 0.2%. At the same time, the change law between foam volume and CFA concentration conforms to the polynomial function $y = 253.71 + 4343.53x - 20{,}402.37x^2 + 40{,}452.20x^3 - 29{,}361.20x^4$, $R^2 = 1.00000$, and the fitting degree is very good, as shown in Figure 7.

3.2. Effect of Foam Stabilizer Concentration and Binder Concentration on Foam Performance. An appropriate amount of foam stabilizer Curdlan added to CFA can effectively enhance its foaming ratio.

When the concentration of foam stabilizer is 2%, the maximum foaming ratio can be increased to 5.8%. The changing law of the relationship between the foam volume and the foam stabilizer conforms to the nonlinear curve function Boltzmann $y = 602.23 - 80533.32/(1 + \exp((x - 4.85)/0.66))$, $R^2 = 0.98877$, and the fitting degree is very well, as shown in Figure 8.

In the concentration range of 1.0−1.8%, from the overall trend of change, the higher the concentration of sodium silicate aqueous solution (SSAS), the greater the viscosity of foam, as shown in Figure 8. The SSAS at the same concentration increases gradually with time, and the foam viscosity increases slowly at first and finally tends to be stable. SSAS can be wrapped around the foam liquid film to form a protective film with a certain strength. This effectively enhances the water

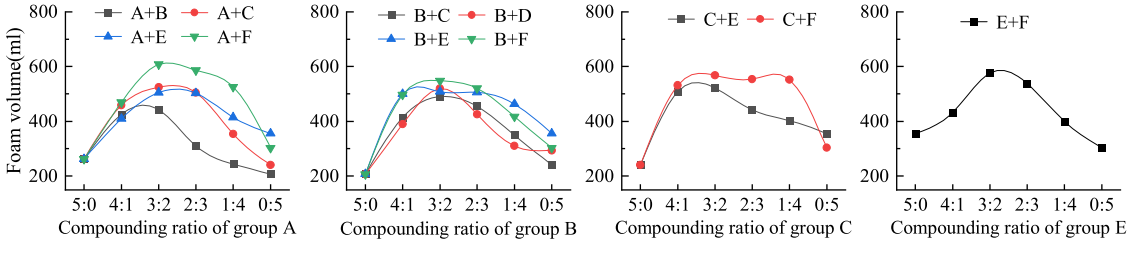

Figure 4. Foam volume under different compounding ratios.

https://doi.org/10.1021/acsomega.3c02881
ACS Omega 2023, 8, 24615−24623

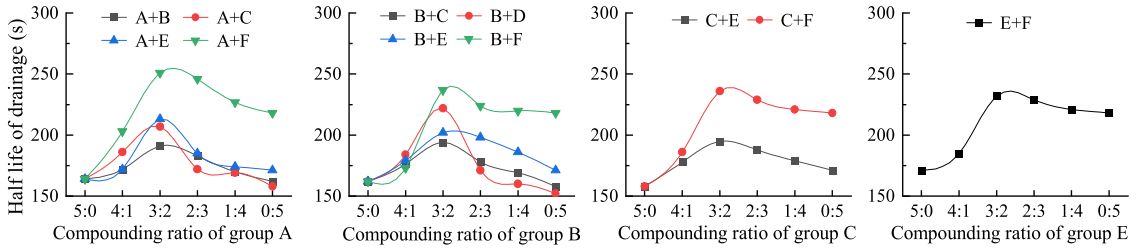

Figure 5. Half-life of liquid drainage under different compound ratios.

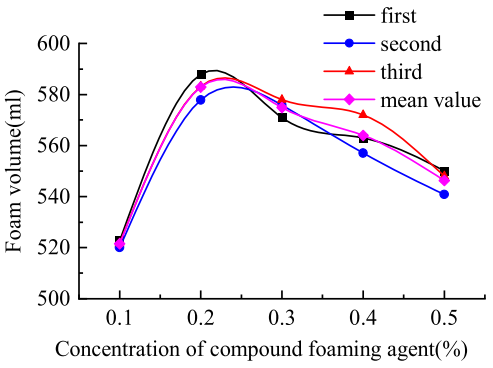

Figure 6. Relationship curve between foam volume and concentration of compound foaming agent.

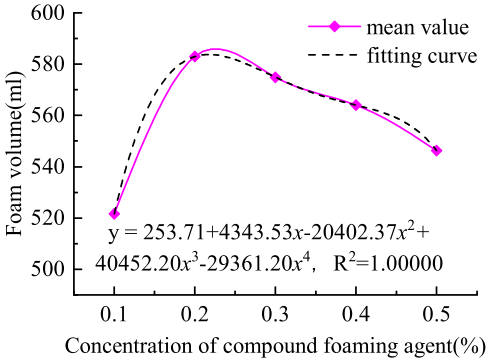

Figure 7. Relationship curve between foam volume and concentration of compound foaming agent.

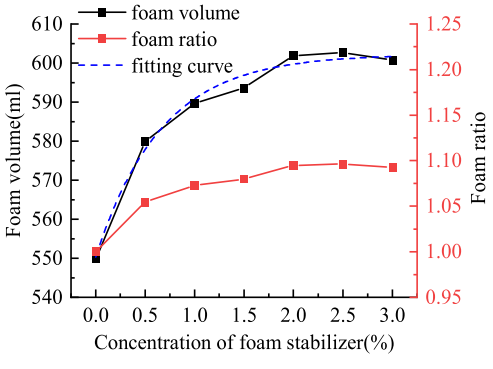

Figure 8. Curve of the relationship between foam volume and foam stabilizer concentration.

retention performance of the foam, reduces its drainage rate, and increases its drainage half-life. With the increase in SSAS concentration, the foam volume gradually decreased and the drainage half-life gradually increased. Considering the volume of foam and the half-life of drainage, it can be concluded that when the concentration of SSAS is 1.6%, the overall foaming performance is optimal, as shown in Figures 9 and 10. At the

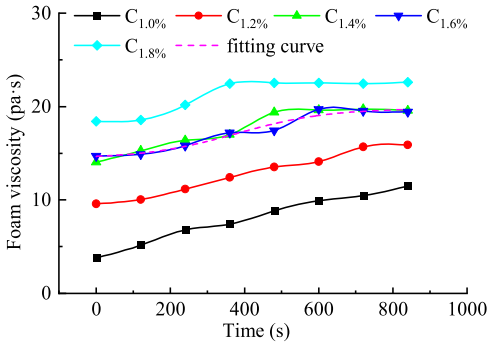

Figure 9. Curves of foam viscosity as a function of binder concentration and time.

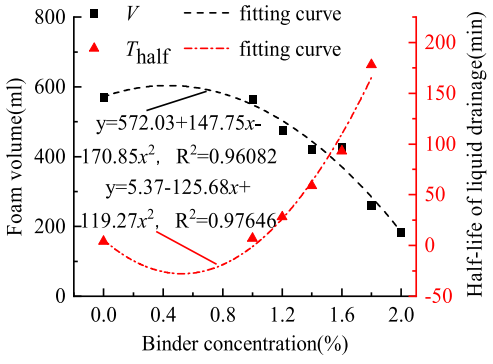

Figure 10. Variation curve of the relationship between binder concentration and foam performance.

same time, when the binder concentration is 1.6%, the relationship between foam viscosity and time changes following the nonlinear curve function Boltzmann $y = 19.81 - 5.38/(1 + \exp((x - 379.43)/122.80))$, $R^2 = 0.96197$, as shown in Figure 9. The relationship between foam volume, drainage half-life, and binder concentration conforms to the polynomial function $y = 572.03 + 147.75x - 170.85x^2$ and $y = 5.37 - 125.68x + 119.27x^2$, respectively, and the fitting degree is good, as shown in Figure 10.

3.3. Effect of Water−Cement Ratio, pH Value, and Temperature on Foam Performance. As the water−cement ratio increases from 3:1 to 6:1, the volume of foam increases from 426 to 486 mL, as shown in Figure 11. This shows that the foaming ability of foam increases with the increase of the water−cement ratio. At the same time, the stability of foam decreases, and the half-life of liquid drainage decreases from 93 to 35 min. The PFA particles adhere to the outer layer of the liquid membrane, forming a support skeleton

https://doi.org/10.1021/acsomega.3c02881
ACS Omega 2023, 8, 24615−24623

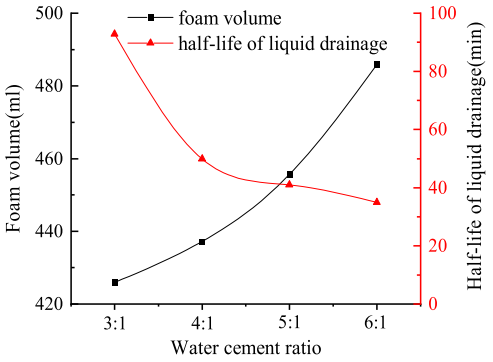

Figure 11. Effect of water−cement ratio on foam properties.

with a certain strength. Therefore, with the increase of the water−cement ratio, the stability of foam becomes worse. In summary, the optimal water−cement ratio for ITPF is 5:1.

When the pH value is between 3 and 11, the foam volume shows a changing trend of first increasing—then decreasing—then increasing—then decreasing, as shown in Figure 11. When the pH value is 9, the maximum foaming volume of foam is 572 mL. At the same time, when the pH value is between 3 and 11, the liquid yield of foam generally shows a changing trend of first decreasing—then increasing—then decreasing—then increasing. When the pH is 9, the maximum amount of liquid separation is 14 mL. To sum up, when the pH value is 9, the water retention effect is the best, the amount of liquid separation is the smallest, and the comprehensive performance of foam is the best, as shown in Figure 12.

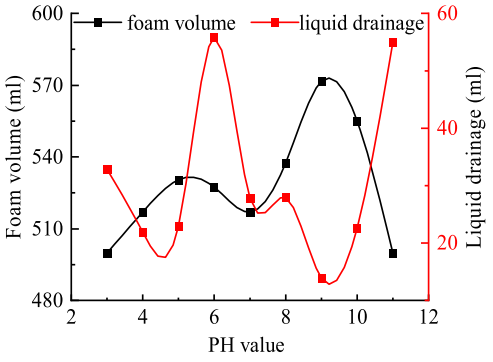

Figure 12. Influence of PH value on the performance of foam.

In the temperature range of 20−60 °C, the volume of foam increases with the increase in temperature. In the range of 60−100 °C, the volume of foam decreases with the increase in temperature. The reason for this phenomenon is that after exceeding 60 °C, the gas inside the ITPF bubble expands due to heat, resulting in a larger bubble volume, reaching its liquid film toughness limit, and starting to crack. At the same time, in the range of 20−100 °C, the change rule of foam volume conforms to the polynomial function $y = 342.79 + 31.27x + 1.97x^2 + 0.06x^3 - 9.57x^4 + 7.29 \times 10^{-6}x^5 - 2.15 \times 10^{-8}x^6$, $R^2 = 0.97073$, and the fitting degree are good, as shown in Figure 13.

3.4. Analysis of Thermogravimetric Test Results.

Under air test conditions, the thermogravimetric test curves of raw coal, AOS + coal, and ITPF + coal are represented by thermogravimetric$_{RC}$ (TG_{RC}), TG_{AOS}, and TG_{ITPF}, respectively, as shown in Figure 14. The TG_{ITPF} curve is used as the

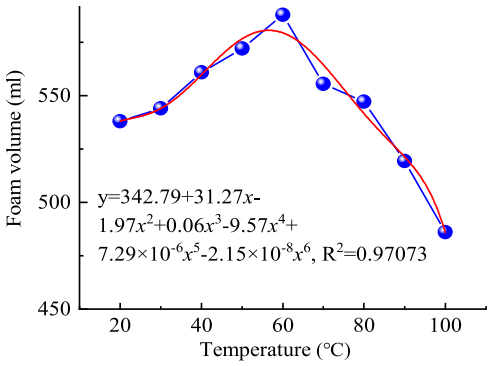

Figure 13. Effect of temperature on foaming performance.

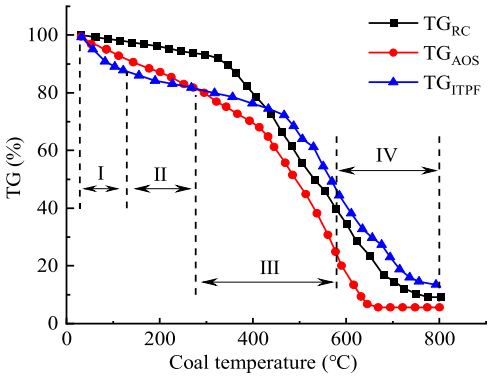

Figure 14. Thermogravimetric test curves of three coal samples.

analysis object. The entire process of coal spontaneous combustion can be divided into four characteristic stages, including the evaporation desorption stage (Stage I), intense oxidation stage (Stage II), accelerated combustion stage (Stage III), and decelerated combustion stage (Stage IV),[45,46] as shown in Figures 14, 15, and 16.

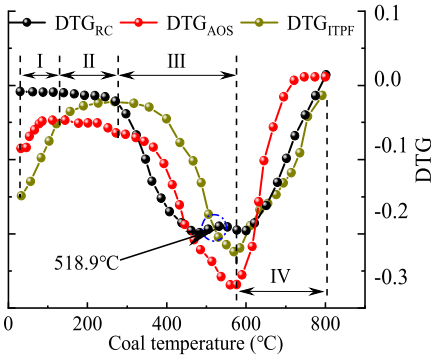

Figure 15. DTG curve of RC + coal, AOS + coal and ITPF + coal at different stages.

At the first stage of the TG_{ITPF} curve (30−129.4 °C), the coal sample starts heating. At this time, the active group in the coal molecular structure undergoes chemical adsorption with O_2. The compound reaction rate of coal and oxygen accelerates, releasing gases such as CO_2, CO, CH_4, etc. Second, the CH_4 and H_2O adsorbed in the coal body are largely desorbed and evaporated during the coal temperature rise, resulting in weight loss of the coal sample.[47,48] At the same temperature, the weight loss rates of the three types of coal are in the order of $DTG_{ITPF} > DTG_{AOS} > DTG_{RC}$, and at

https://doi.org/10.1021/acsomega.3c02881
ACS Omega 2023, 8, 24615−24623

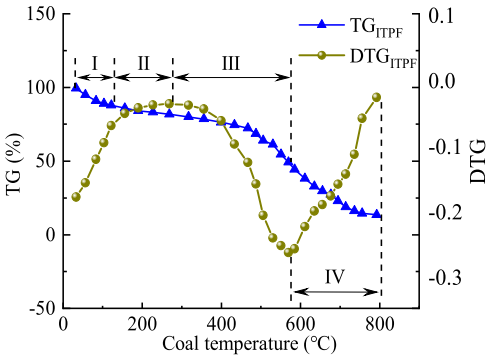

Figure 16. TG, DTG, curve of ITPF + coal at different stages.

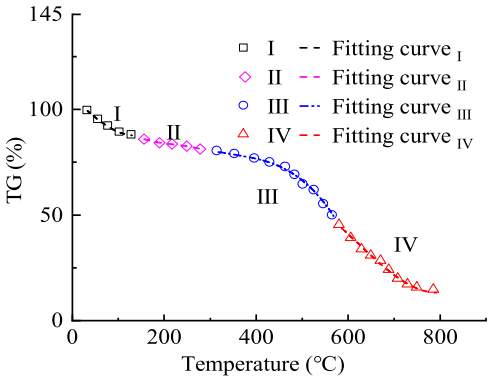

Figure 17. TG segmented fitting curve of ITPF + coal.

the same time, as shown in Figure 15. In Phase I, ITPF + coal has the greatest mass loss. The reason is that the ITPF+coal has a higher water content percentage, as shown in Figures 14 and 16.

At the second stage of the TG_{ITPF} curve (129.4−277.0 °C), the chemical reaction of coal oxygen is relatively intense. The fracture rate of aromatic structures in coal molecules is accelerated. The number of active groups increased sharply and the heat release increased rapidly. At this stage, there is no phenomenon of oxygen uptake and weight gain. This is because ITPF adheres to the surface of coal, isolating it from oxygen. The rate at which coal absorbs oxygen is less than the rate at which gas escapes from the coal oxidation reaction. At the same time, the order of weight loss rates of the three types of coal has changed $DTG_{AOS} > DTG_{ITPF} > DTG_{RC}$, at the same temperature, as shown in Figure 15. When the coal temperature continues to increase, the coal enters the third (accelerated combustion) stage. Before and after 579.5 °C, the weight loss rates of the three coal samples reached a peak, as shown in Figure 15.

At the third stage of the TG_{ITPF} curve (277.0−579.5 °C), the rate of coal weight loss increases rapidly. Before and after 579.5 °C, the weight loss rates of the three coal samples reached a peak, as shown in Figure 15. In the range of 277.0−518.9 °C, the weight loss rate of ITPF + coal is always the smallest $DTG_{ITPF} < DTG_{AOS}$ or $DTG_{ITPF} < DTG_{RC}$, as shown in Figure 15. This indicates that within this temperature range, ITPF has the best fire prevention and extinguishing effects, and can effectively inhibit coal combustion. After the weight loss rate of the coal sample reaches a peak, it begins to enter the fourth (decelerated combustion) stage.

At the fourth stage of the TG_{ITPF} curve (579.5−800.0 °C), the rate of coal weight loss gradually decreases. In the range of 579.5−800.0 °C, the weight loss rate of ITPF + coal is greater than that of raw coal $DTG_{ITPF} > DTG_{RC}$. At this moment, ITPF has lost its fire prevention and extinguishing effectiveness.

In summary, ITPF has the best fire prevention and extinguishing effect in the accelerated combustion stage of coal(III). At the same time, the fitting formulas for the TG curve of ITPF + coal in stages I to IV all conform to the polynomial function $y = A + B_1x + B_2x^2 + B_3x^3$, and all fitting degrees R^2 are greater than 0.994, as shown in Figure 17 and Table 2.

3.5. Analysis on Test Results of Coal Spontaneous Combustion Tendency. The spontaneous combustion tendency of raw coal, AOS + coal, and ITPF + coal is tested using a spontaneous combustion tester. The same test conditions were set, with a column box temperature of 30 °C, a thermal conductivity temperature of 80 °C, an empty tube adsorption time of 5 min, an empty tube gas carrying capacity of 32 cm^3/min, and an empty tube adsorption gas flow of 20 cm^3/min. The results of the oxygen absorption test and analysis for coal are shown in Table 3 and Figure 17.

Table 2. Segmental Fitting Function of TG Curve of ITPF + Coal

serial number	stage	fitting formula	R^2
I	evaporation desorption	$y = 105.73 - 1.99 \times 10^{-1}x - 1.44 \times 10^{-3}x^2 - 3.68 \times 10^{-6}x^3$	0.99994
II	intense oxidation	$y = 128.39 - 5.62 \times 10^{-1}x + 2.43 \times 10^{-3}x^2 - 3.67 \times 10^{-6}x^3$	0.99635
III	accelerated combustion	$y = 178.95 - 7.89 \times 10^{-1}x - 2.16 \times 10^{-3}x^2 - 2.05 \times 10^{-6}x^3$	0.99577
IV	decelerated combustion	$y = -412.72 - 2.57x - 4.46 \times 10^{-3}x^2 - 2.396 \times 10^{-6}x^3$	0.99453

Table 3. Test and Result Analysis of Oxygen Absorption Capacity of Coal

name of sample	carrier gas flow cm^3/min	adsorption gas flow cm^3/min	oxygen uptake cm^3/g	auto-ignition level
raw coal	32.4	19.9	0.79 > 0.70	class I
AOS + coal	31.7	20	0.40 < 0.47 ≤ 0.70	class II
ITPF + coal	6.2	19.9	0.29 ≤ 0.40	class III

The oxygen absorption capacities of raw coal, AOS + coal, and ITPF + coal are 0.79, 0.47, and 0.29 cm^3/g, respectively, as shown in Figure 18. Their corresponding spontaneous combustion tendencies are Class I prone to spontaneous

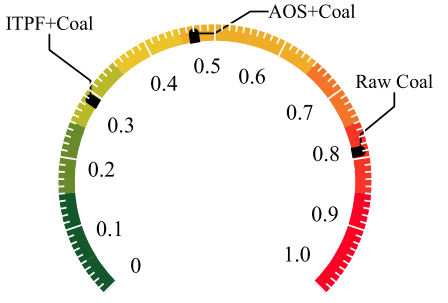

Figure 18. Classification Diagram of Coal Spontaneous Combustion Tendency.

https://doi.org/10.1021/acsomega.3c02881
ACS Omega 2023, 8, 24615−24623

combustion, Class II prone to spontaneous combustion, and Class III nonprone to spontaneous combustion. The above analysis shows that the spontaneous combustion tendency of coal samples treated with ITPF is reduced from Class I easy to spontaneous combustion to Class III not easy to spontaneous combustion, and the flame-retardant effect is significant.

4. CONCLUSIONS

To develop a pollution-free flame-retardant foam with high foaming properties and good stability, we selected CFA as the surfactant, Curdlan as the foam stabilizer, and sodium silicate as the binder and determined the optimal concentration of the three components through experiments. Simultaneously, the effects of water−cement ratio, pH, and temperature on the performance of ITPF were tested. Second, using the TG test and coal spontaneous combustion tendency test, the different characteristics of raw coal, AOS + coal, and ITPF + coal were investigated from two aspects: thermal weight loss rate and unit oxygen uptake of coal. The conclusions are as follows:

(1) The optimal CFA combination and ratio test scheme were designed according to the test method of dual group compounding. The CFA components SDBS and AOS with high foaming ratio and good stability of foam were determined, and the ratio was SDBS/AOS (3:2) by experimental method. The concentration of CFA was 0.2%, the concentration of stabilizer Curdlan was 0.5%, and the concentration of binder sodium silicate was 1.6%.

(2) In the third stage of accelerated coal combustion, the coal sample weight loss rate DTGITPF is less than DTG_{AOS} or DTG_{RC} within the range of 277.0 to 518.9 °C. ITPF can effectively inhibit the combustion of coal and has the best fire prevention and extinguishing effect. ITPF has the best fire prevention and extinguishing effect, which can effectively inhibit the combustion of coal at this stage.

(3) The fitting formulas for the thermogravimetric curve TG_{ITPF} of ITPF + coal samples at stages I to IV conform to the polynomial function $y = A + B_1x + B_2x^2 + B_3x^3$, and the fitting degree R^2 is greater than 0.994.

(4) ITPF can effectively isolate the contact between coal and oxygen, physically preventing the spontaneous combustion of coal. ITPF can effectively inhibit the coal oxygen complex reaction and reduce the tendency of coal spontaneous combustion. After the coal sample is treated with ITPF, the spontaneous combustion tendency is reduced from Class I easy to spontaneous combustion to Class III not easy to spontaneous combustion, and the flame-retardant effect is significant.

AUTHOR INFORMATION

Corresponding Author

Baoshan Jia − *School of Safety Science and Engineering, Liaoning Technical University, Fuxin, Liaoning 123000, China; Key Laboratory of Mine Thermo-Motive Disaster and Prevention, Ministry of Education, Liaoning Technical University, Huludao, Liaoning 125105, China*; Email: jbs1972@126.com

Authors

Jian Chen − *School of Safety Science and Engineering, Liaoning Technical University, Fuxin, Liaoning 123000, China; Key Laboratory of Mine Thermo-Motive Disaster and Prevention, Ministry of Education, Liaoning Technical University, Huludao, Liaoning 125105, China*; orcid.org/0000-0003-2600-6374

Shuoqin Fu − *School of Safety Science and Engineering, Liaoning Technical University, Fuxin, Liaoning 123000, China; Key Laboratory of Mine Thermo-Motive Disaster and Prevention, Ministry of Education, Liaoning Technical University, Huludao, Liaoning 125105, China*

Ying Wen − *School of Mining Engineering, Liaoning Technical University, Fuxin, Liaoning 123000, China*

Yuntao Liang − *State Key Laboratory of Coal Mine Safety Technology, China Coal Technology & Engineering Group Protection Research Institute, Fushun, Liaoning 113122, China*

Fuchao Tian − *State Key Laboratory of Coal Mine Safety Technology, China Coal Technology & Engineering Group Protection Research Institute, Fushun, Liaoning 113122, China*

Complete contact information is available at: https://pubs.acs.org/10.1021/acsomega.3c02881

Notes

The authors declare no competing financial interest.

ACKNOWLEDGMENTS

The authors acknowledge the support provided by the National Natural Science Foundation of China (grant numbers 52174229 and 52174230).

REFERENCES

(1) Lü, H. F.; Xiao, Y.; Deng, J.; Li, D. J.; Yin, L.; Shu, C. M. Inhibiting effects of 1-butyl-3-methyl imidazole tetrafluoroborate on coal spontaneous combustion under different oxygen concentrations. *Energy* **2019**, *186*, No. 115907.

(2) Mrabet, Z.; Alsamara, M.; Saleh, A. S.; Anwar, S. Urbanization and non-renewable energy demand: A comparison of developed and emerging countries. *Energy* **2019**, *170*, 832−839.

(3) Zhang, Y. T.; Shi, X. Q.; Li, Y. Q.; Liu, Y. R. Characteristics of carbon monoxide production and oxidation kinetics during the decaying process of coal spontaneous combustion. *Can. J. Chem. Eng.* **2018**, *96*, 1752−1761.

(4) Guanhua, N.; Qian, S.; Meng, X.; Hui, W.; Yuhang, X.; Weimin, C.; Gang, W. Effect of NaCl-SDS compound solution on the wettability and functional groups of coal. *Fuel* **2019**, *257*, No. 116077.

(5) Deng, J.; Yang, Y.; Zhang, Y. N.; Liu, B.; Shu, C. M. Inhibiting effects of three commercial inhibitors in spontaneous coal combustion. *Energy* **2018**, *160*, 1174−1185.

(6) Li, P.; Yang, Y.; Li, J.; Miao, G.; Zheng, K.; Wang, Y. Study on the oxidation thermal kinetics of the spontaneous combustion characteristics of water-immersed coal. *Thermochim. Acta* **2021**, *699*, No. 178914.

(7) Bai, Z.; Wang, C. P.; Deng, J.; Kang, F.; Shu, C. M. Experimental investigation on using ionic liquid to control spontaneous combustion of lignite. *Process Saf. Environ. Prot.* **2020**, *142*, 138−149.

(8) Chao, J. K.; Chu, T. X.; Yu, M. G.; Han, X. F.; Hu, D. M.; Liu, W.; Yang, X. L. An experimental study on the oxidation kinetics characterization of broken coal under stress loading. *Fuel* **2021**, *287*, No. 119515.

(9) Deng, J.; Chen, W. L.; Wang, C. P.; Wang, W. F. Prediction Model for Coal Spontaneous Combustion Based on SA-SVM. *ACS Omega* **2021**, *6*, 11307−11318.

(10) Xu, Q.; Yang, S. Q.; Yang, W. M.; Tang, Z. Q.; Hu, X. C.; Song, W. X.; Zhou, B. Z. Micro-structure of crushed coal with different

metamorphic degrees and its low-temperature oxidation. *Process Saf. Environ. Prot.* **2020**, *140*, 330−338.
(11) Lu, Y.; Shi, S. L.; Wang, H. Q.; Tian, Z. J.; Ye, Q.; Niu, H. Y. Thermal characteristics of cement microparticle-stabilized aqueous foam for sealing high-temperature mining fractures. *Int. J. Heat Mass Transfer* **2019**, *131*, 594−603.
(12) Shi, Q. L.; Qin, B. T. Experimental research on gel-stabilized foam designed to prevent and control spontaneous combustion of coal. *Fuel* **2019**, *254*, No. 115558.
(13) Zhao, J. Y.; Deng, J.; Wang, T.; Song, J. J.; Zhang, Y. N.; Shu, C. M.; Zeng, Q. Assessing the effectiveness of a high-temperature-programmed experimental system for simulating the spontaneous combustion properties of bituminous coal through thermokinetic analysis of four oxidation stages. *Energy* **2019**, *169*, 587−596.
(14) Tang, Y. B.; Wang, H. E. Experimental investigation on microstructure evolution and spontaneous combustion properties of secondary oxidation of lignite. *Process Saf. Environ. Prot.* **2019**, *124*, 143−150.
(15) Zhang, Y. T.; Li, Y. Q.; Huang, Y.; Li, S. S.; Wang, W. F. Characteristics of mass, heat and gaseous products during coal spontaneous combustion using TG/DSC−FTIR technology. *J. Therm. Anal. Calorim.* **2018**, *131*, 2963−2974.
(16) Han, C.; Nie, S. B.; Liu, Z. G.; Liu, S.; Zhang, H.; Li, J. Y.; Zhang, H. R.; Wang, Z. H. A novel biomass sodium alginate gel foam to inhibit the spontaneous combustion of coal. *Fuel* **2022**, *314*, No. 122779.
(17) Xi, Z. L.; Wang, X. D.; Wang, X. L.; Wang, L.; Li, D.; Guo, X. Y.; Jin, L. W. Polymorphic foam clay for inhibiting the spontaneous combustion of coal. *Process Saf. Environ. Prot.* **2019**, *122*, 263−270.
(18) Shao, Z. L.; Wang, D. M.; Wang, Y. M.; Zhong, X. X.; Tang, X. F.; Hu, X. M. Controlling coal fires using the three-phase foam and water mist techniques in the Anjialing Open Pit Mine. China. *Nat. Hazards* **2015**, *75*, 1833−1852.
(19) Zhang, Q.; Hu, X. M.; Wu, M. Y.; Zhao, Y. Y.; Yu, C. Effects of different catalysts on the structure and properties of polyurethane/water glass grouting materials. *J. Appl. Polym. Sci.* **2018**, *135*, No. 46460.
(20) Huang, Z. A.; Yan, L. K.; Zhang, Y. H.; Gao, Y. K.; Liu, X. H.; Liu, Y. Q.; Li, Z. Y. Research on a new composite hydrogel inhibitor of tea polyphenols modified with polypropylene and mixed with halloysite nanotubes. *Fuel* **2019**, *253*, 527−539.
(21) Qin, B. T.; Dou, G. L.; Wang, Y.; Xin, H. H.; Ma, L. Y.; Wang, D. M. A superabsorbent hydrogel−ascorbic acid composite inhibitor for the suppression of coal oxidation. *Fuel* **2017**, *190*, 129−135.
(22) Li, Q.-W.; Xiao, Y.; Zhong, K.; Shu, C.; Lü, H.; Deng, J.; Wu, S. Overview of commonly used materials for coal spontaneous combustion prevention. *Fuel* **2020**, *275*, No. 117981.
(23) Huang, Z.; Song, D.; Zhang, Y.; Yin, Y.; Hu, X.; Gao, Y.; Yang, Y.; Tian, Y. Characterization and performance testing of an intumescent nanoinhibitor for inhibiting coal spontaneous combustion. *ACS Omega* **2022**, *7*, 17202−17214.
(24) Lu, Y. Laboratory study on the rising temperature of spontaneous combustion in coal stockpiles and a paste foam suppression technique. *Energy Fuels* **2017**, *31*, 7290−7298.
(25) Qin, B.; Wang, H.; Yang, J.; Liu, L. Large-area goaf fires: a numerical method for locating high-temperature zones and assessing the effect of liquid nitrogen fire control. *Environ. Earth Sci.* **2016**, *75*, No. 1396.
(26) Tian, Z. J.; Lu, Y.; Liu, S. M.; Shi, S. L.; Li, H.; Ye, Q. Application of inorganic solidified foam to control the coexistence of unusual methane emission and spontaneous combustion of coal in the Luwa coal mine, China. *Combust. Sci. Technol.* **2020**, *192*, 638−656.
(27) Zhang, L. L.; Wu, W. J.; Wei, J.; Bian, Y. P.; Luo, H. G. Preparation of foamed gel for preventing spontaneous combustion of coal. *Fuel* **2021**, *300*, No. 121024.
(28) Zhi, G. J.; Xie, R.; Yang, R. G.; Cui, J. Q.; An, X. Y.; Zhang, Y. L. Study on the preparation of montmorillonite-type multiple network composite gel for coal spontaneous combustion and its firefighting mechanism. *ACS Omega* **2023**, *8*, 10493−10502.
(29) Zhang, X.; Pan, Y. Preparation, properties and application of gel materials for coal gangue control. *Energies* **2022**, *15*, No. 557.
(30) Qin, B. T.; Ma, D.; Li, F. L.; Li, Y. Aqueous clay suspensions stabilized by alginate fluid gels for coal spontaneous combustion prevention and control. *Environ. Sci. Pollut. Res.* **2017**, *24*, 24657−24665.
(31) Wang, G.; Yan, G. Q.; Zhang, X. H.; Du, W. Z.; Huang, Q. M.; Sun, L. L.; Zhang, X. Q. Research and development of foamed gel for controlling the spontaneous combustion of coal in coal mine. *J. Loss Prev. Process Ind.* **2016**, *44*, 474−486.
(32) Xi, X.; Jiang, S. G.; Shi, Q. L.; Yin, C. C. Experimental investigation on the leakage plugging and fire extinguishment characteristics of industrial solid waste-based composite foam slurry materials. *Energy* **2023**, *269*, No. 126780.
(33) Xue, D.; Hu, X. M.; Cheng, W. M.; Wei, J. F.; Zhao, Y. Y.; Shen, L. Fire prevention and control using gel-stabilization foam to inhibit spontaneous combustion of coal: Characteristics and engineering applications. *Fuel* **2020**, *264*, No. 116903.
(34) Guo, Q.; Ren, W. X.; Zhu, J. T.; Shi, J. T. Study on the composition and structure of foamed gel for fire prevention and extinguishing in coal mines. *Process Saf. Environ. Prot.* **2019**, *128*, 176−183.
(35) Xi, Z. L.; Li, D.; Feng, Z. Y. Characteristics of polymorphic foam for inhibiting spontaneous coal combustion. *Fuel* **2017**, *206*, 334−341.
(36) Zheng, X. Z.; Zhang, D.; Wen, H. Design and performance of a novel foaming device for plugging air leakage in underground coal mines. *Powder Technol.* **2019**, *344*, 842−848.
(37) Yang, J. Q.; Li, Q.; Li, M.; Zhu, W. B.; Yang, Z. J.; Qu, W. Q.; Hu, Y. C.; Li, H. L. In Situ Decoration of Selenide on Copper Foam for the Efficient Immobilization of Gaseous Elemental Mercury. *Environ. Sci. Technol.* **2020**, *54*, 2022−2030.
(38) Sharma, S.; Patel, R. H. Novel carbon foam composites reinforced with carbon fiber felt developed from inexpensive pitch precursor matrix. *J. Compos. Mater.* **2020**, *54*, 3559−3569.
(39) Yan, B. R.; Hu, X. M.; Cheng, W. M.; Zhao, Y. Y.; Wang, W.; Liang, Y. T.; Liu, T. Y.; Feng, Y.; Xue, D. A novel intumescent flame-retardant to inhibit the spontaneous combustion of coal. *Fuel* **2021**, *297*, No. 120768.
(40) Sun, H. J.; Zeng, L.; Peng, T. J. Research status and progress of high-value utilization of coal fly ash. *Mater. Rep.* **2021**, *35*, 3010−3015.
(41) Lin, S. D.; Jiang, X. G.; Zhao, Y. M.; Yan, J. H. Zeolite greenly synthesized from fly ash and its resource utilization: A review. *Sci. Total Environ.* **2022**, *851*, No. 158182.
(42) Li, X. Y.; Bai, C. Y.; Qiao, Y. J.; Wang, X. D.; Yang, K.; Colombo, P. Preparation, properties and applications of fly ash-based porous geopolymers: A review. *J. Cleaner Prod.* **2022**, *359*, No. 132043.
(43) Wang, N. N.; Sun, X. Y.; Zhao, Q.; Yang, Y.; Wang, P. Leachability and adverse effects of coal fly ash: A review. *J. Hazard. Mater.* **2020**, *396*, No. 122725.
(44) Wang, C.; Xu, G. G.; Gu, X. Y.; Gao, Y. H.; Zhao, P. High value-added applications of coal fly ash in the form of porous materials: A review. *Ceram. Int.* **2021**, *47*, 22302−22315.
(45) Jia, H. L.; Cui, B.; Jiao, Z. Y.; Zhao, W. L.; Xu, Q. Q.; Sun, F. N. Study on the whole process and gas products of coal-oxygen complex reaction based on TG/DSC/MS technology. *J. China Coal Soc.* **2022**, *47*, 3704−3714.
(46) Zhang, X. H.; Bai, Y. E.; Li, Y. Q.; Ma, T. Kinetics and segmentation law of coal oxidation at elevated temperature. *Xi'an Keji Daxue Xuebao* **2017**, *37*, 474−478.
(47) Xue, D.; Hu, X. M.; Cheng, W. M.; Wu, M. Y.; Shao, Z. A.; Li, Y. S.; Zhao, Y. Y.; Zhang, K. Carbon dioxide sealing-based inhibition of coal spontaneous combustion: A temperature-sensitive micro-encapsulated fire-retardant foamed gel. *Fuel* **2020**, *266*, No. 117036.
(48) Wang, K.; Han, T.; Deng, J.; Zhang, Y. N. Comparison of combustion characteristics and kinetics of jurassic and carboniferous-permian coals in China. *Energy* **2022**, *254*, No. 124315.

https://doi.org/10.1021/acsomega.3c02881
ACS Omega 2023, 8, 24615−24623